JM2, encoding a fork head–related protein, is mutated in X-linked autoimmunity–allergic disregulation syndrome

Talal A. Chatila,[1,2] Frank Blaeser,[1] Nga Ho,[1] Howard M. Lederman,[3] Constantine Voulgaropoulos,[4] Cindy Helms,[5] and Anne M. Bowcock[1,5,6]

[1]Department of Pediatrics, and
[2]Department of Pathology and Immunology and the Center for Immunology, Washington University School of Medicine, St. Louis, Missouri 63110, USA
[3]Department of Pediatrics, Johns Hopkins University School of Medicine, Baltimore, Maryland 21287, USA
[4]PEDCare Inc., St. Louis, Missouri 63141, USA
[5]Department of Genetics, and
[6]Department of Internal Medicine, Washington University School of Medicine, St. Louis, Missouri 63110, USA

Address correspondence to: Talal Chatila, Division of Immunology/Rheumatology, Department of Pediatrics, Washington University School of Medicine, 660 S. Euclid Avenue, Box 8208, St. Louis, Missouri 63110, USA. Phone: (314) 286-2883; Fax: (314) 286-2895; E-mail: chatila@kids.wustl.edu.

X-linked autoimmunity–allergic disregulation syndrome (XLAAD) is an X-linked recessive immunological disorder characterized by multisystem autoimmunity, particularly early-onset type 1 diabetes mellitus, associated with manifestations of severe atopy including eczema, food allergy, and eosinophilic inflammation. Consistent with the allergic phenotype, analysis of two kindreds with XLAAD revealed marked skewing of patient T lymphocytes toward the Th2 phenotype. Using a positional-candidate approach, we have identified in both kindreds mutations in *JM2*, a gene on Xp11.23 that encodes a fork head domain–containing protein. One point mutation at a splice junction site results in transcripts that encode a truncated protein lacking the fork head homology domain. The other mutation involves an in-frame, 3-bp deletion that is predicted to impair the function of a leucine zipper dimerization domain. Our results point to a critical role for *JM2* in self tolerance and Th cell differentiation.

Introduction

An X-linked recessive syndrome of autoimmunity, allergic disregulation, and diarrhea has been recognized in several families (1–6) (Mendelian Inheritance in Man entries 304930, 304790). This syndrome, referred to herein as XLAAD (for X-linked autoimmunity–allergic disregulation syndrome), presents early in life with autoimmunity, severe allergic inflammation, secretory diarrhea, and failure to thrive (1–6). Many affected males suffer from classical type 1 diabetes mellitus that frequently presents in the immediate postnatal period or early infancy. Type 1 diabetes mellitus in XLAAD is characterized by islet cell destruction by infiltrating T cells and, in some cases, by autoantibody formation (7). Patients with XLAAD also manifest a more general predilection to autoimmune diseases including autoimmune polyendocrinopathies (especially thyroiditis), hemolytic anemia, thrombocytopenia, and enteropathy. Severe allergic inflammation in XLAAD patients is reflected by the occurrence of eczema, food allergy, elevated IgE levels, and peripheral eosinophilia. Many patients suffer from persistent secretory diarrhea, which may be caused by both food allergy–associated eosinophilic gastroenteropathy and

autoimmune enteropathy. Susceptibility to recurrent staphylococcal infections has been variably described in some XLAAD patients and may reflect the well-known association of staphylococcal infections with severe eczema. XLAAD is frequently fatal, due to unrelenting diarrhea and wasting, difficult-to-treat diabetes, and/or superimposed infections.

XLAAD has been previously mapped in two unrelated kindreds to Xp11.23–Xq13.3 (6, 8). We have studied two additional kindreds with XLAAD and have mapped the XLAAD locus to an overlapping region on the X chromosome. We report the identification by a positional-candidate approach of a gene encoding a fork head homology domain–related protein that is targeted by mutations in XLAAD patients.

Methods

Clinical material. Peripheral blood samples were obtained for study. Informed consent was obtained from all study participants or their legal guardians.

DNA and RNA isolation. Lymphocytes isolated from whole blood were used to generate phytohemagglutinin-driven (PHA-driven) T-cell lines and Epstein-Barr virus–transformed B-cell lines. DNA was extracted with

Table 1
Primers used in analysis of *JM2* genomic and cDNA sequences

	Forward primer	Reverse primer
Genomic DNA Primer		
Exon 1	TGATCACACTCCTGGACTCG	GAAGGCGAGAAGTGGGTAGA
Exon 2	CGTGTGACTCCTTTCCCCTA	ACAGTAAAGGTCGGCACCTG
Exon 3	CCCACTTACAGGCACTCCTC	CTGCTCACAGCCAAGGATCT
Exon 4	GCTCAAAATGAGAGGCCTTG	CCACTTGCAGACACCATTTG
Exon 5	CACCTTCCCAAATCCCAGT	TATTGGGATGAAGCCTGAGC
Exon 6	GTTAAGGGAACGAGGGGTGT	GGTTTTGCGCACTATCCCTA
Exon 7	GGATAGGGATAGTGCGCAAA	CAGTCTGAGTCTGCCACCAC
Exon 8	GGCGACAGAGCAAGACTCA	CCCAGAGCCTGTCAGGATTA
Exon 9	GTGGACACGGGTGTTGACGG	GGCACTCAGAGGGAGACAGG
Exons 10 and 11	CCCCACATCTAGTCCTGTCC	TGTTCGTCCATCCTCCTTTC
cDNA primers (nested PCR)		
Outer pair (bp 41–59; 1140–1121)	CACCCAAAGCCTCAGACCT	CCAGGTGTAGGGTTGGAACA
Inner pair (bp 353–72; 1102–1083)	TCTGCACCTTCCCAAATCCC	TCCGTTTCTTGCGGAACTCC
Inner pair (bp 639–59; 1036–1014)	AATGGCACTGACCAAGGCTTC	CAAAGCACTTGTGCAGACTCAG

Puregene kit (Gentra Systems Inc., Minneapolis, Minnesota, USA), and total RNA was obtained using the Trizol Reagent (Life Technologies Inc., Rockville, Maryland, USA). cDNA was made using AMV–reverse transcriptase (Promega Corp., Madison, Wisconsin, USA).

Mapping of XLAAD candidate interval. Genotyping of microsatellite markers in patients and their family members was accomplished using standard PCR primers and methods for the ABI 377 DNA sequencer (Applied Biosystems, Foster City, California, USA). Resulting data were processed through the ABI program Genotyper, to determine marker alleles for each family member. LOD-SCORE (option of LINKAGE program) was used to determine possible linkage to the X chromosome markers: DXS1223, DXS1068, DXS6810, DXS7132, DXS6800, DXS6789, DXS6797, DXS1047, and DXS7127, which cover an estimated 76 cM interval on the X chromosome on the sex-averaged Marshfield map.

Candidate gene identification. Genes in the syntenic human region of the *Scurfy* critical interval were identified by searching public domain data bases. Homology searches for candidate transcriptional regulators were carried out by BLAST search (www.ncbi.nlm.nih.gov). Two leading candidate transcriptional regulators were identified within the syntenic human region of the Scurfy mouse: *Tcfe3*, whose deficiency leads to a phenotype distinct from *Scurfy* (9), and *JM2*. The gene sequence of *JM2* has been previously established as part of the human genome sequencing project (GenBank accession no. AF235097). The genomic sequence was originally predicted to encode 10 exons corresponding to a 1326-bp open reading frame (accession no. NM_014009). However, comparison of predicted exon 10 sequence with sequences of RT-PCR–amplified transcripts of normal individuals confirmed the presence of a small intron within predicted exon 10 (bp 58622–58443 of AF235097; 997–1176 of NM_014009). The corrected open reading frame sequence is 1146 bp long encoding a 381–amino acid protein.

Mutation detection. PCR primers used to amplify individual *JM2* exons from genomic DNA and *JM2* transcripts from T lymphoblast–derived cDNA are listed in Table 1. PCR amplification of genomic sequences was carried out by heating the reaction mix at 95°C for 1 minute followed by 35 cycles with the following settings: 94°C for 15 seconds, 60°C for 30 seconds, and 72°C for 30 seconds. Amplified products were sequenced with an ABI 377 sequencer with labeled di-deoxy terminators. Nested PCR amplification of cDNA sequences was carried out using cDNA derived from total RNA of T lymphoblasts by reverse transcription. A first-step PCR reaction was carried out using outer primers (bp 41–59; 1140–1121). PCR conditions were 95°C for 1 minute followed by 35 cycles with the following settings: 94°C for 30 seconds, 58°C for 1 minute, and 72°C for 1

Table 2
Clinical characteristics of XLAAD patients

Clinical feature	Patients
Failure to thrive	5/5
Eczema	4/5
Food allergy	5/5
High IgE levels	4/5
Type 1 diabetes mellitus	5/5
Chronic diarrhea	5/5
Autoimmune cytopenia	3/5

Figure 1

Haplotype analysis of pedigrees XLAAD-100 and XLAAD-200. Circles, females; squares, males. Filled symbols, affected individuals; open symbols, unaffected individuals; forward slash through symbol, deceased individual. X chromosome haplotypes are schematically represented by side bars, while numbers next to the side bars represent the sizes (in bp) of alleles of markers listed in the inset. XLAAD-200-16, -17, -18, and -29 died of fetal hydrops. A question mark refers to deceased males whose genotype could not be determined. Haplotypes for X chromosome markers are shown. A crossover proximal to marker DXS1068 in individual XLAAD-200-4 defines DXS1223 as the proximal flanking marker for XLAAD, and a second recombination in XLAAD-200-27 distal to DXS6800 defines DXS6789 as the distal flanking marker for the XLAAD locus.

XLAAD-100

XLAAD-200

Loci
DXS1223
DXS1068
DXS6810
DXS7132
DXS6800
DXS6789
DXS6797
DXS1047
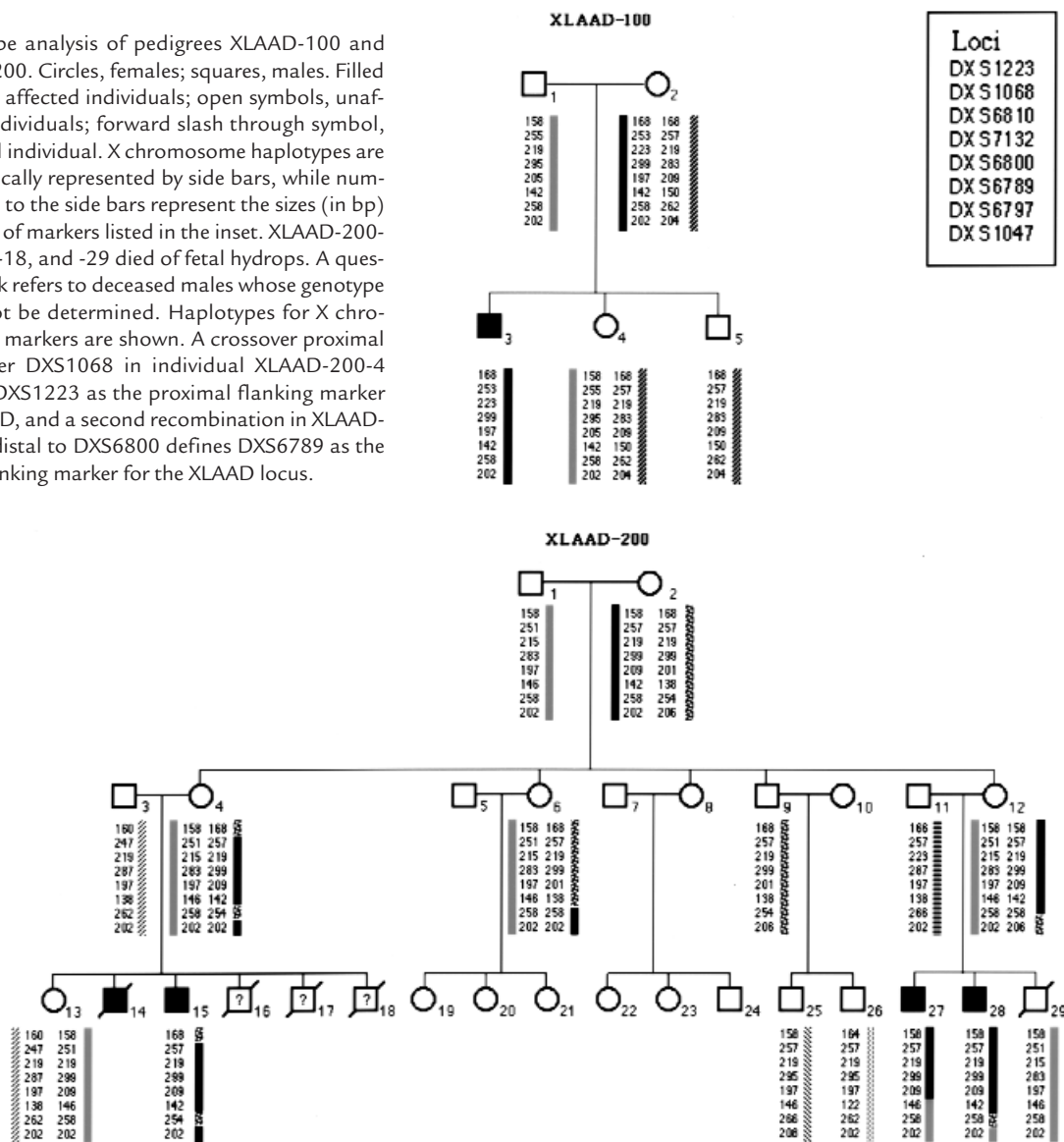
minute. An aliquot of the first PCR reaction mix was then used as template for the second PCR reaction, which was run under the same conditions except for annealing temperatures of 60°C for primers bp 353–372; 1102–1083 (for detection of exon 7 mutation) and 65°C for primers bp 639–659; 1036–1014 (for detection of exon 9 skipping).

RNase protection assay. Peripheral blood mononuclear cells of patients and male controls were stimulated with PHA for 5 days. The lymphoblasts were either left untreated or activated with phorbol ester and calcium ionophore for 1 hour, as indicated. Total RNA was isolated and examined for cytokine expression by RNase protection assay using the Multi-Probe Hck-1 Kit (Pharmingen, San Diego, California, USA).

Results and Discussion

We studied two families (referred to as XLAAD-100 and -200) with a total of five affected males, one in XLAAD-100 and four in XLAAD-200 (Figure 1). All affected children suffered from type 1 diabetes mellitus with onset in infancy (range 3 weeks to 11 months), chronic diarrhea, and allergic reactions especially to foods (Table 2). Other family members, including obligate heterozygote female carriers of the XLAAD-200 kindred, were clinically unaffected. Laboratory studies revealed evidence of heightened allergic reactivity including eosinophilia and elevated IgE levels, as well as positive radioallergosorbent tests and positive immediate hypersensitivity responses by skin prick tests to food and other allergens. After in vitro stimulation of peripheral blood lymphocytes with mitogens, there was exaggerated expression of the Th2 cytokines IL-4, IL-5, IL-10, and IL-13 and decreased expression of the Th1 cytokine IFN-γ (Figure 2). Both the clinical phenotype and the laboratory studies were consistent with dysregulated Th cell type 2 responses in XLAAD.

The XLAAD susceptibility locus was mapped by

Figure 2

Enhanced Th2 cytokine expression in T lymphocytes of XLAAD patients. RNase protection assay analysis of cytokine gene expression in control and patient PHA-derived T-cell lymphoblasts is shown. Peripheral blood mononuclear cells of XLAAD-100 index case (patient 1) and XLAAD-200-27 (patient 2) and their respectively related healthy male controls were stimulated with PHA for 5 days. The resultant lymphoblasts were either left untreated (Medium) or activated with phorbol ester (PMA) and calcium ionophore (Iono) for 1 hour, as indicated. Total RNA was isolated and examined for cytokine expression by RNase protection assay using a commercially available kit (Pharmingen). L32 and GAPDH are transcripts of household genes that are used as internal controls. Results are representative of three different experiments.
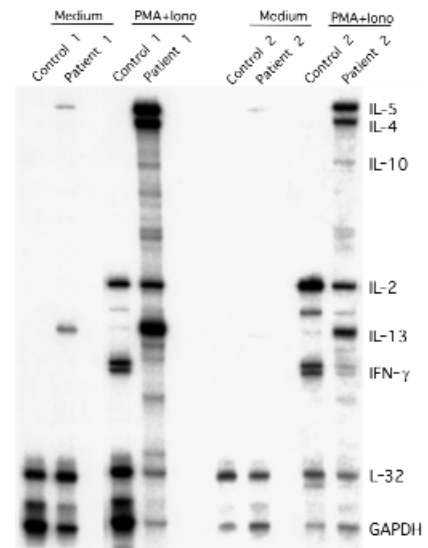
screening the probands and their relatives with polymorphic markers from the X chromosomes. Two-point linkage analysis mapped the XLAAD locus to a 46 cM interval that is flanked by the polymorphic markers DXS1223 proximally and DXS6789 distally, with a lod score of 1.81 at DXS6810 (Figure 1). This interval overlaps those previously defined in other XLAAD families. Importantly, the XLAAD interval overlaps with the critical interval of the Scurfy mouse gene, a murine model of dysregulated lymphocyte activation (10). *Scurfy* exhibits several XLAAD-related features, including T-cell hyperactivation and enhanced Th2 cytokine production, cytopenia, eczema, and diarrhea (11, 12). This suggested that alterations in the human homologue of the mouse gene responsible for the *Scurfy* mutation may also be responsible for XLAAD.

The critical region of *Scurfy* has been localized to a <300 kb segment on chromosome Xp11.23–p11.22 (13, 14). Accordingly, coding sequences in the public domain that map to the syntenic human region were systematically screened for candidate XLAAD genes. Given evidence of enhanced Th2 lymphokine gene transcription, particular emphasis was placed on screening either established or candidate transcriptional regulators, the latter identified by BLAST search. *JM2*, encoding a candidate transcription factor of previously unknown function, was identified in the syntenic human region of the *Scurfy* critical interval. The *JM2* open reading frame is long and is predicted to encode a 381-amino-acid-long protein that contains a fork head homology domain. This is a highly conserved DNA-binding domain that defines the HNF-3/fork
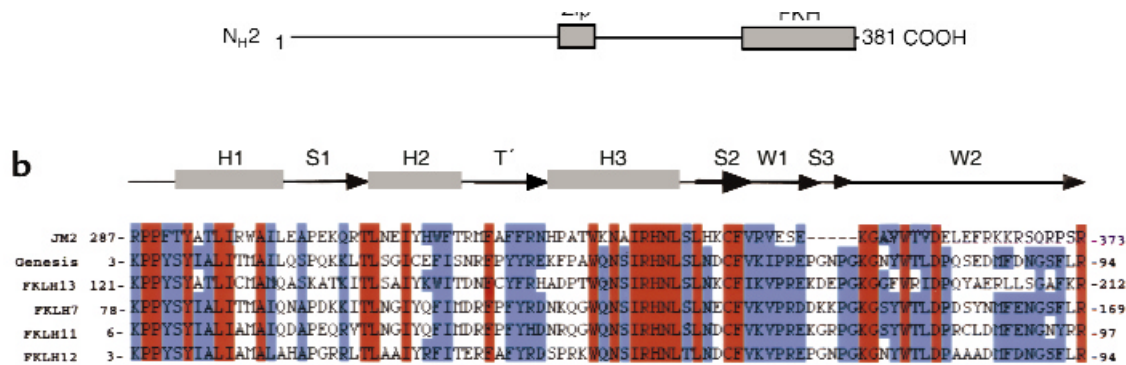
Figure 3

Structural features of JM2 protein. (**a**) Domain organization. A leucine zipper (Zip) domain is present halfway through the protein at amino acids 189–210, while the fork head homology domain (FKH) extends from amino acids 287–373. (**b**) Homology of JM2 fork head domain sequence with fork head domains of other proteins including the Drosophila transcription factor Genesis and the human fork head related–proteins FKLH13, 7, 11, and 12. Red color indicates residue identity, while green indicates homology. Homology was established by searching the Conserved Domain Database (www.ncbi.nlm.nih.gov/Structure/), and alignment was accomplished using the Clustalw program (www.ebi.ac.uk/clustalw/). The organization of a canonical fork head domain is schematically illustrated. It includes three α helices (H1, 2, and 3), and a connecting loop (T´). Three β strands (S1, 2, and 3), and two wings (W1 and 2) arranged in order (H1-S1-H2-T´-H3-S2-W1-S3-W2) (15, 16).

head family of transcription factors and is characterized by distinct winged helix structure (15, 16) (Figure 3). JM2 is distinguished from other fork head homology proteins by the location of the fork head homology domain at the carboxyl-terminus and by the additional presence of a leucine zipper (Zip) dimerization domain midway through the protein (Figure 3). A putative nuclear localization signal is found at the carboxyl-terminus.

The critical role played by fork head homology and Zip domains in JM2 function was highlighted by the mutations found in the two XLAAD kindreds. Genomic DNA sequencing of the XLAAD-100 proband revealed the presence of an A→G substitution at position +4 of the 5′ donor splice junction of IVS9 (Figure 4a). This substitution was not present in the child's two other siblings or his parents, including his mother, indicating that it arose de novo. It was also lacking in 100 X chromosomes screened for this mutation. Sequence analysis of RT-PCR–amplified JM2 mRNA transcripts revealed skipping of *JM2* exon 9 in transcripts of the index case of family XLAAD-100 but not in unaffected family members or in unrelated controls (Figure 4, b and c). Exon 9 skipping results in a frame shift at codon 273 that gives rise to a premature stop signal at codon 286. This leads to the generation of a truncated JM2 protein that lacks the fork head homology domain (Figure 4d). When the RT-PCR was run at a less stringent annealing temperature (60°C instead of 65°C), a second minor RT-PCR product appeared. This product, which migrated slower than its wild-type counterpart, resulted from aberrant splicing at IVS9 5′ donor splice junction (data not shown). No wild-type product was detected under any of the RT-PCR conditions tried. These results confirmed the pathogenicity of IVS9 +4 A→G mutation due to its disruption of IVS9 5′ donor splice junction.

Analysis of the XLAAD-200 kindred revealed affected males to suffer from a 3-bp deletion in *JM2* exon 7, resulting in an in-frame deletion of bp 600–602 of JM2 cDNA (Figure 5a). Mothers of affected males, as well as the grandmother, were heterozygous for the mutant allele, while unaffected family members and control subjects lacked this mutation. There was in XLAAD-200 an unexpectedly high incidence of fatal hydrops fetalis. In one tested baby (XLAAD-200-29), the JM2 gene was normal; the others (XLAAD-200-16, -17, -18) were not available for testing.

The mutant transcripts are predicted to encode a JM2 protein lacking glutamic acid 201 residue (ΔE201). This residue lies in the second of the three heptad repeats that constitute the JM2 Zip motif. The JM2 Zip motif is most closely related to the three-heptad Zip motif of N-myc, with virtual identity at the second heptad (17) (Figure 5). Previous studies have revealed an essential role for the N-myc Zip motif and its individual heptad repeats including the second heptad in N-myc homodimerization and in heterodimerization of N-myc with its partner protein Max (18, 19). Specifi-
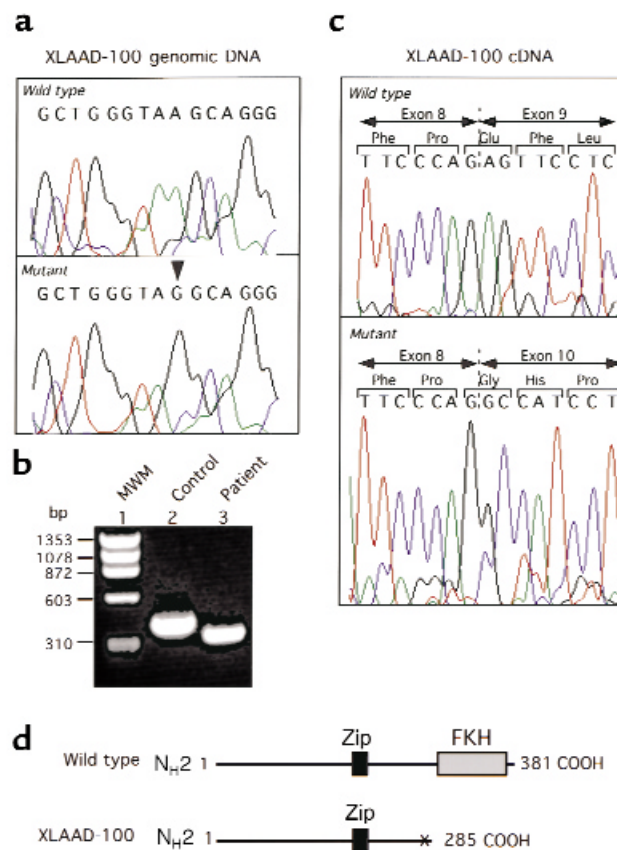

Figure 4
Identification of a 5′ splice junction mutation in JM2 IVS9 of XLAAD-100 index case. (**a**) Analysis of JM2 IVS9 5′ splice junction site sequence in the index case and his sibling brother control. An A→G transition at position +4 of the 5′ splice junction site is noted in the patient sequence (indicated by an arrowhead). (**b** and **c**) Exon 9 skipping in XLAAD-100 index case. (**b**) RT-PCR analysis of JM2 open reading frame 3′ end (bp 639–1036) in patient and control mRNA transcripts, revealing faster migration of patient RT-PCR product on agarose gel electrophoresis as compared with control product. MWM, molecular weight markers. (**c**) Sequence analysis of RT-PCR products shown in **b**, confirming the presence of exon 9 deletion and frame shift alteration in patient sequence. (**d**) Schematic representation of predicted mutant JM2 protein product in XLAAD-100 index case, showing truncation of the protein just before the fork head homology domain.

cally, alteration of the N-myc second heptad by mutagenesis of the distal leucine residue to proline or by mutagenesis of the glutamic-lysine-glutamic (EKE) motif to alanine residues impairs homo/heterodimerization and homodimerization, respectively (19). By analogy, it is speculated that the ΔE201 deletion may interfere with heterodimerization of JM2 with partner proteins and/or its homodimerization, resulting in failure of effector function.

Studies on the Scurfy mouse have confirmed that disease pathogenesis is mediated by CD4+ T helper cells (20–22). The disease can be induced by transfer of Scurfy CD4+ T cells to normal hosts, and it is cured upon breeding of Scurfy mice into T cell–deficient
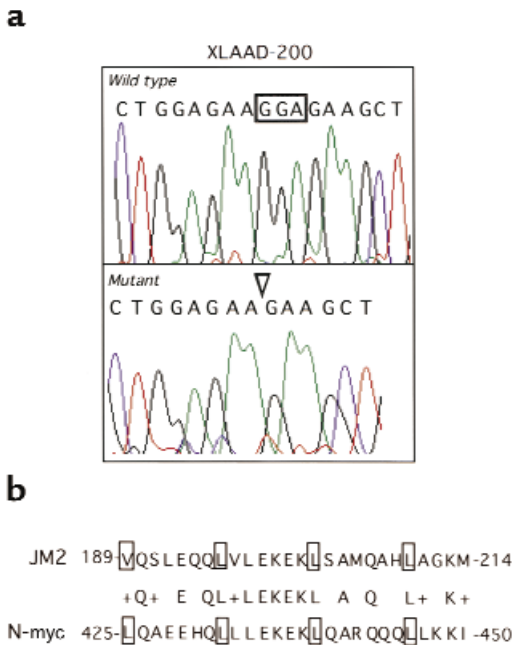
Figure 5

Identification of a 3-bp deletion in exon 7 of affected XLAAD-200 individuals. (**a**) Analysis of amplified genomic exon 7 sequence of XLAAD-200-28 and his sibling control XLAAD-200-29 showing deletion of bp 15–17 in the patient's exon 7 sequence. The same mutation was confirmed by cDNA sequencing (data not shown). (**b**) Schematic representation of JM2 Zip domain and its homology to the Zip domain of human N-myc. The deleted glutamic residue (E), located in the second heptad, is boldface. A plus sign indicates homologous amino acid residues.

mouse strains (20–22). This and clinical observations in XLAAD patients of the beneficial effects of T-cell immunosuppressants point to a pivotal role for *JM2* in maintaining T-cell tolerance and in regulating Th cell differentiation. The unusual association of XLAAD with type 1 diabetes mellitus and with intense allergic inflammation distinguishes *JM2* from other genes whose dysfunction results in autoimmunity, including those encoding complement proteins and components of the Fas cell death pathway, and *AIRE*, the defective gene in autoimmune polyendocrinopathy-candidiasis-ectodermal dystrophy (APECED) (23–26). It will be important to determine the mechanism(s) by which *JM2* regulates autoimmunity and Th cell differentiation, including its role in maintaining central versus peripheral tolerance and in regulating well-described transcriptional programs underlying Th cell lineage commitment (27).

The high incidence of type 1 diabetes mellitus in XLAAD patients, which is 100% in affected males of several XLAAD families, indicates that *JM2* deficiency functions as a highly penetrant single gene trigger of type 1 diabetes mellitus. Of note, there exists a male bias in the incidence of sporadic type 1 diabetes mellitus, estimated at a male-to-female ratio of 1.7, which has been linked to a susceptibility locus on Xp11 that includes *JM2* (28). This suggests that mutations and/or

polymorphisms in *JM2* may more broadly contribute to the pathogenesis of sporadic type 1 diabetes mellitus. *JM2* may also interact with other previously established susceptibility genes for type 1 diabetes mellitus such as HLA-DR genes, a premise suggested by the observation that male bias and linkage to Xp11 in sporadic type 1 diabetes mellitus is most prominent in HLA-DR3+ individuals (28). These issues will need to be addressed in broad-based population studies on sporadic type 1 diabetes mellitus.

1. Powell, B.R., Buist, N.R., and Stenzel, P. 1982. An X-linked syndrome of diarrhea, polyendocrinopathy, and fatal infection in infancy. *J. Pediatr.* **100**:731–737.
2. Satake, N., et al. 1993. A Japanese family of X-linked auto-immune enteropathy with haemolytic anaemia and polyendocrinopathy. *Eur. J. Pediatr.* **152**:313–315.
3. Roberts, J., and Searle, J. 1995. Neonatal diabetes mellitus associated with severe diarrhea, hyperimmunoglobulin E syndrome, and absence of islets of Langerhans. *Pediatr. Pathol. Lab. Med.* **15**:477–483.
4. Peake, J.E., McCrossin, R.B., Byrne, G., and Shepherd, R. 1996. X-linked immune dysregulation, neonatal insulin dependent diabetes, and intractable diarrhoea. *Arch. Dis. Child. Fetal Neonatal Ed.* **74**:F195–F199.
5. Di Rocco, M., and Marta, R. 1996. X linked immune dysregulation, neonatal insulin dependent diabetes, and intractable diarrhoea. *Arch. Dis. Child. Fetal Neonatal Ed.* **75**:F144.
6. Ferguson, P.J., et al. 2000. Manifestations and linkage analysis in X-linked autoimmunity-immunodeficiency syndrome. *Am. J. Med. Genet.* **90**:390–397.
7. Cilio, C.M., et al. 2000. Congenital autoimmune diabetes mellitus. *N. Engl. J. Med.* **342**:1529–1531.
8. Bennett, C.L., et al. 2000. X-linked syndrome of polyendocrinopathy, immune dysfunction, and diarrhea maps to Xp11.23-Xq13.3. *Am. J. Hum. Genet.* **66**:461–468.
9. Merrell, K., et al. 1997. The absence of the transcription activator TFE3 impairs activation of B cells in vivo. *Mol. Cell. Biol.* **17**:3335–3344.
10. Godfrey, V.L., Wilkinson, J.E., and Russell, L.B. 1991. X-linked lymphoreticular disease in the scurfy (sf) mutant mouse. *Am. J. Pathol.* **138**:1379–1387.
11. Lyon, M.F., Peters, J., Glenister, P.H., Ball, S., and Wright, E. 1990. The scurfy mouse mutant has previously unrecognized hematological abnormalities and resembles Wiskott-Aldrich syndrome. *Proc. Natl. Acad. Sci. USA.* **87**:2433–2437.
12. Kanangat, S., et al. 1996. Disease in the scurfy (sf) mouse is associated with overexpression of cytokine genes. *Eur. J. Immunol.* **26**:161–165.
13. Blair, P.J., et al. 1994. The mouse scurfy (sf) mutation is tightly linked to Gata1 and Tfe3 on the proximal X chromosome. *Mamm. Genome.* **5**:652–654.
14. Means, G.D., Toy, D.Y., Baum, P.R., and Derry, J.M. 2000. A transcript map of a 2-Mb BAC contig in the proximal portion of the mouse X chromosome and regional mapping of the scurfy mutation. *Genomics.* **65**:213–223.
15. Kaufmann, E., and Knochel, W. 1996. Five years on the wings of fork head. *Mech. Dev.* **57**:3–20.
16. Gajiwala, K.S., and Burley, S.K. 2000. Winged helix proteins. *Curr. Opin. Struct. Biol.* **10**:110–116.
17. Kohl, N.E., et al. 1986. Human N-myc is closely related in organization and nucleotide sequence to c-myc. *Nature.* **319**:73–77.
18. Wenzel, A., Cziepluch, C., Hamann, U., Schurmann, J., and Schwab, M. 1991. The N-Myc oncoprotein is associated in vivo with the phosphoprotein Max(p20/22) in human neuroblastoma cells. *EMBO J.* **10**:3703–3712.
19. Ma, A., et al. 1993. DNA binding by N- and L-Myc proteins. *Oncogene.*

8:1093–1098.

20. Blair, P.J., et al. 1994. CD4+CD8- T cells are the effector cells in disease pathogenesis in the scurfy (sf) mouse. *J. Immunol.* **153**:3764–3774.
21. Godfrey, V.L., Rouse, B.T., and Wilkinson, J.E. 1994. Transplantation of T cell-mediated, lymphoreticular disease from the scurfy (sf) mouse. *Am. J. Pathol.* **145**:281–286.
22. Clark, L.B., et al. 1999. Cellular and molecular characterization of the scurfy mouse mutant. *J. Immunol.* **162**:2546–2554.
23. Colten, H.R., and Rosen, F.S. 1992. Complement deficiencies. *Annu. Rev. Immunol.* **10**:809–834.
24. Straus, S.E., Sneller, M., Lenardo, M.J., Puck, J.M., and Strober, W. 1999. An inherited disorder of lymphocyte apoptosis: the autoimmune lymphoproliferative syndrome. *Ann. Intern. Med.* **130**:591–601.
25. Finnish-German APECED Consortium. 1997. An autoimmune disease, APECED, caused by mutations in a novel gene featuring two PHD-type zinc-finger domains. The Finnish-German APECED Consortium. Autoimmune Polyendocrinopathy-Candidiasis-Ectodermal Dystrophy. *Nat. Genet.* **17**:399–403.
26. Nagamine, K., et al. 1997. Positional cloning of the APECED gene. *Nat. Genet.* **17**:393–398.
27. Glimcher, L.H., and Murphy, K.M. 2000. Lineage commitment in the immune system: the T helper lymphocyte grows up. *Genes Dev.* **14**:1693–1711.
28. Cucca, F., et al. 1998. A male-female bias in type 1 diabetes and linkage to chromosome Xp in MHC HLA-DR3-positive patients. *Nat. Genet.* **19**:301–302.